

DOI: 10.20514/2226-6704-2020-10-5-357-371

V.S. Petrovichev¹, A.V. Melekhov^{*1,2}, M.A. Sayfullin^{1,2,3}, I.G. Nikitin^{1,2}¹ — National Medical Research Center of Treatment and Rehabilitation of the Russian Healthcare Ministry, Moscow, Russia² — Pirogov Russian National Research Medical University, Moscow, Russia³ — Gamaleya National Research Center for Epidemiology and Microbiology of the Russian Healthcare Ministry, Moscow, Russia

The Role of Computed Tomography in Differentiation of Coronavirus Pneumonia, its Complications and Comorbidities. Case Reports

Abstract

Background: computer tomography (CT) features of COVID-19, their temporal changes and differences from other pulmonary (viral and bacterial pneumonia) and non-pulmonary diseases are well described in recent publications. The prevalence and characteristics of signs of concomitant problems that could be identified at chest CT are less studied. **Aim:** to analyze the prevalence and characteristics of chest CT features of COVID-19, its complications and comorbidities. **Methods:** retrospective analysis of CT and clinical data of 354 patients hospitalized with suspected COVID at April and May of 2020. **Results:** 962 CT scans were analyzed (3 (2-3) scans per patient). First CT was performed at 8 (5-11) day of sickness. Several roentgenological scenarios could be highlighted: patients with coronavirus pneumonia (n=295; 83%); with combination of COVID-19 and another pathology (n=36; 10%); with complications of COVID-19 (n=12; 3%); with alternative pathology (n=2; 1%); without any pathological signs (n=9; 3%). Several cases, illustrating CT signs of coronavirus pneumonia, its complications and comorbidities are reported. **Conclusion:** CT possibilities are not limited to detect typical COVID-19 signs, it also helps to differentiate pulmonary and other thoracic pathology.

Key words: COVID-19, coronavirus pneumonia, multispiral computed tomography, differentiation of complications and comorbidities

Conflict of interests

The authors declare no conflict of interests

Sources of funding

The authors declare no funding for this study

Article received on 01.09.2020

Accepted for publication on 28.09.2020

For citation: Petrovichev V.S., Melekhov A.V., Sayfullin M.A. et al. The Role of Computed Tomography in Differentiation of Coronavirus Pneumonia, its Complications and Comorbidities. Case Reports. The Russian Archives of Internal Medicine. 2020; 10(5): 357-371. DOI: 10.20514/2226-6704-2020-10-5-357-371

ACVE — acute cerebrovascular event, ARDS — acute respiratory distress syndrome, AV — artificial ventilation, BMI — body mass index, BP — blood pressure, CHF — chronic heart failure, CI — confidence interval, COVID-19 — new coronavirus infection, CRP — C-reactive protein, CT — computed tomography, EF — ejection fraction, HR — heart rate, IQR — interquartile range, LDH — lactate dehydrogenase, LV — left ventricle, PCR — polymerase chain reaction, RF — respiratory failure, RNA — ribonucleic acid, RR — respiratory rate, SARS-CoV-2 — severe acute respiratory syndrome-related coronavirus 2

*Contacts: Alexandr V. Melekhov, e-mail: avmelekhov@gmail.com
ORCID ID: <https://orcid.org/0000-0002-1637-2402>

Introduction

The first reports of the novel coronavirus disease (COVID-19) emerged in late December 2019 from Wuhan, Hubei, China. The report described four cases of pneumonia of unknown etiology; standard 3–5 day antibacterial treatment was ineffective [4]. On January 7, 2020, the World Health Organization published information on the identity of the novel coronavirus that caused this disease. It also linked this infection with a visit to a market in Wuhan [2, 3]. Subsequently, the affinity of the virus to the receptors of angiotensin-converting enzyme 2 in alveolocytes was established, followed by the infection of cells and a direct cytopathic effect [4, 5]. Due to its clinical features and genetic relationship with the coronavirus that caused the 2002–2003 SARS outbreak, this virus was named SARS-CoV-2 [6]. From January to June 2020, an exponential increase in incidence was observed worldwide; the number of cases exceeded 7 million. The first reports based on the description of individual clinical cases emerged in early January. Cases of pneumonia associated with the new coronavirus were described as bilateral interstitial lung disease, resistant to standard antibiotic treatment, with increasing respiratory failure (RF) and acute respiratory distress syndrome (ARDS).

The significant rise in the number of patients facilitated the rapid accumulation of experience in assessing, diagnosing, and treating COVID-19 patients. The first generalized study based on the examination of 1,099 patients established the frequency of various clinical symptoms and patterns on the computed tomography (CT) of the chest [7]. In particular, CT changes were found in 86.2% of 975 examined patients. Bilateral changes were found in 51.8% of patients, and the most common symptom of ground-glass opacity — in 56.4%. The key point in CT diagnostics was the staging of changes; the stages corresponded to the days of disease [8]. Later, several variants of differentiation of CT images of COVID-19 were proposed both according to the criteria of compliance (bilateral lesion, ground-glass opacity, crazy-paving pattern, etc.) and according to the dynamic changes described in various literature reviews [9–11]. There is a common opinion about the significantly lower sensitivity of chest X-ray

compared with CT. As there is no correlation of auscultatory signs of pneumonia with the volume of the lung lesion and the frequently false-negative primary results of polymerase chain reaction (PCR), CT became a reference method for the diagnosis of COVID-19 and disease severity. CT is also recommended as a screening examination in Russia [12].

The massive spread of COVID-19 naturally led to the involvement in the epidemic process of people with bronchopulmonary pathologies caused by other diseases, including cancer and tuberculosis [13, 14], which raised the need for differential diagnosis. Besides COVID-19, more than 400 cases of community-acquired pneumonia are recorded per 100 thousand population in Russia annually. Tuberculosis is common — 44.06 per 100 thousand population [15]. More than 60 thousand new cases of malignant neoplasms of the trachea, bronchi and lungs are reported annually [16]. Consequently, radiologists and clinicians have to differentiate coronavirus pneumonia from other respiratory diseases that can often be underlying (Table 1).

Numerous publications describe the differential diagnosis of X-ray symptoms of COVID-19, their specificity, incidence in different variants of the course of coronavirus disease, differences from other types of pulmonary lesions (other viral or bacterial pneumonias), and non-pulmonary diseases [20]. In real clinical practice, coronavirus pneumonia can develop in comorbid patients with radiological signs of other diseases. We could not find in the available medical literature any works on the analysis of the incidence and characteristics of the radiological signs of concomitant diseases in patients with coronavirus disease.

Problems of differential diagnosis in patients with COVID-19 are not only of clinical but also epidemiological significance since timely and competent interpretation of CT data allows to separate patient flows to different departments of medical institutions. In this regard, a number of clinical cases reported at the Federal State Budgetary Institution “Scientific Research Treatment and Rehabilitation Center of the Ministry of Health of the Russian Federation (FSBI “SRC TRC of the Ministry of Health of Russia) during the reprofiling period in April–June 2020 are of interest.

Table 1. Differential-diagnostic spectrum of symptoms detected by CT CT in patients with coronavirus infection [17-19]

Symptom	Morphological substrate and frequency in COVID-19	Detection in other diseases
Groud glass opacity	Inflammation of the alveolar septa with intraalveolar cellular desquamation 88%	Other viral pneumonia Pneumocystis pneumonia Fungal pneumonia Paracancrotic pneumonia Eosinophilic pneumonia Organizing pneumonia Idiopathic hypereosinophilic syndrome ARDS (Acute Respiratory Distress Syndrome) Cardiogenic pulmonary edema Hypersensitivity pneumonitis Lipoid pneumonitis Post-radiation pneumonitis Drug-Induced Lung Disorders Glandular cancer Sarcoidosis Pulmonary vasculitis Alveolar proteinosis
Thickening of the interlobular septa (reticular pattern)	The connecting link between ground glass symptom and consolidation. Interstitial lymphocytic infiltration 50-61,6%	Pulmonary edema Lymphogenous metastasis of glandular cancer
Crazy paving	«Frosted glass» in combination with a reticular pattern (thickening of the interlobular and intralobular interstitium) 89%	Other viral pneumonia Paracancrotic pneumonia Pneumocystis pneumonia Interstitial pneumonia Organizing pneumonia Eosinophilic pneumonia ARDS (Acute Respiratory Distress Syndrome) Pulmonary edema Sarcoidosis Alveolar proteinosis Pulmonary vasculitis Glandular cancer Lipoid pneumonitis Post-radiation pneumonitis
Consolidation	Complete replacement of alveolar air with exudate 63,9-96%	Bacterial pneumonia Organizing pneumonia Infiltrative tuberculosis Tumors and metastases
Air bronchogram (pneumo-bronchogram)	Air-filled bronchi with consolidation 44,7-56,2%	Bacterial pneumonia Interstitial pneumonia Idiopathic Pulmonary Fibrosis Glandular cancer Cirrhosis of the lung lobe Organizing pneumonia Pulmonary bleeding Tension pneumothorax Tension hydrothorax Pulmonary edema Lung infarction

Table 1 (the end)

Symptom	Morphological substrate and frequency in COVID-19	Detection in other diseases
Halo	The focus of consolidation, surrounded by «frosted glass». Not specific for COVID-19 11,3-17,6%	Other viral infections Fungal infections Metastases of glandular cancer Vasculitis with Wegener's granulomatosis Cryptogenic organizing pneumonia
Reverse (reverse) halo («atoll») symptom	A rounded frosted glass focus surrounded by an annular consolidation. Not specific for COVID-19	Cryptogenic organizing pneumonia Pneumocystis pneumonia Vasculitis with Wegener's granulomatosis Pulmonary tuberculosis Lymphatic granulomatosis Lipoid pneumonitis Lung infarction Post-radiation pneumonitis Tumors and metastases
Bronchiectasis	Progressive and irreversible expansion of the bronchi with or without wall thickening. With COVID-19, a sign of the progression of the infection, detected at the most advanced stages, is detected in 52,5%	COPD Bacterial pneumonia Pulmonary tuberculosis Traction bronchiectasis (pulmonary fibrosis) Kartagener's syndrome Primary immunodeficiencies Alpha-1-antitrypsin deficiency Cystic fibrosis Airway obstruction (foreign body or mass) Systemic lupus erythematosus, rheumatoid arthritis Measles
Cavitation	An insulated, gas-filled cavity inside the seal. With COVID-19, it is detected in the late stages of the disease, showing the progression of the inflammatory process. One of the least frequent CT findings	Lung abscess Primary lung cancer (predominantly squamous cell) Metastases of squamous cell, glandular cancer, sarcoma Pulmonary tuberculosis Septic embolus Rare fungal infections of the lungs Rheumatoid nodules Vasculitis with Wegener's granulomatosis Lung infarction Pneumatocele after trauma (pseudocavity) Pulmonary sequestration Bronchogenic cyst Cystic adenomatoid malformation
Lymphadenopathy	It is observed with the progression of COVID-19, more often with severe forms	Bacterial pneumonia Tuberculosis of the intrathoracic lymph nodes Oncological diseases Lymphoproliferative Disorders Sarcoidosis
Pleural and pericardial effusion	Increased permeability of the pleural vessels, increased hydrostatic pressure in them. One of the rarest signs of COVID-19, more common in critical patients	Pleurisy of other etiology Chronic heart failure Oncological diseases

Materials and Methods

A retrospective analysis of medical records and computed tomograms of patients was carried out, with a description of individual clinical cases, which limited the use of statistical methods. We evaluated 354 patients (age 59 (IQR: 49–70) years old, 56% women) who were hospitalized with suspected COVID-19. The patients were hospitalized from the 1st to the 56th day from the onset of symptoms (8 (IQR: 6–11) days); in 5 (1.4%) patients, the time of disease onset could not be established because verbal contact was impossible.

Each patient admitted to the hospital with suspected COVID-19 was scanned on the same 64-slice CT scanner (Discovery CT750HD; GE Healthcare) located in the “red zone” of the tomography unit. Most of the studies were native with the following parameters: voltage — 100 mA, current — 100 kV, maximum field of view during scanning (up to 50 cm), rotation time — 0.6 s and pitch — 1.375: 1. Slice thickness was 1.25 mm with a 40 cm field of view and a 512 × 512 matrix. Besides, two series of images with different stiffness factors were obtained after reconstruction — in lung and mediastinal windows.

Subsequent post-processing and detailed analysis of thin slice scans with multiplanar reconstructions, in minimum (MinIP) and maximum intensity (MIP) modes were performed remotely via a local area network by a radiologist in the “green zone” of

the department, using Advantage Workstation 4.6 (GE Healthcare, USA).

When assessing changes in the lung parenchyma in patients, physicians relied on the temporary guidelines for the prevention, diagnosis and treatment of the novel coronavirus disease (COVID-19) of the Russian Ministry of Health that were relevant at the time of the study [12]. According to these data, disease severity was assessed based on the size of the lesion (in %) of the lung parenchyma. For a structured assessment of the specificity of changes found in lung tissue, the CO-RADS classification developed by the COVID-19 working group of the Dutch Radiological Society was used [21].

Statistical data processing was performed via SPSS Statistics software. Data are presented as median and interquartile range (IQR); for proportions, a 95% confidence interval (95% CI) is given.

Results

A total of 962 examinations conducted on 354 patients were analyzed; 867 (90.1%) of them were performed at the Treatment and Rehabilitation Center (TRC) and 95 (9.9%) at other hospitals prior to hospitalization at the TRC. The frequency of CTs for one patient was 3 (IQR: 2–3); 25 (7.1%) patients underwent CT only once. The first CT was conducted on the 8th day (IQR: 5–11) from the onset of symptoms (including studies conducted in an outpatient setting).

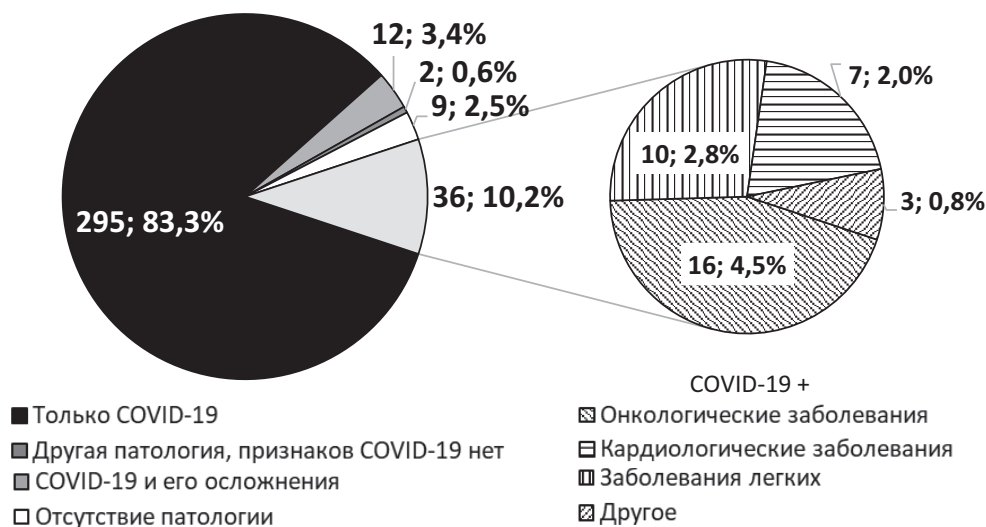


Figure 1. Proportion of patients with computer tomography (CT) features of COVID-19 pneumonia, its complications, comorbidities and alternative diseases, n,%.

Radiological signs observed in patients with COVID-19 during the whole course of disease allow us to divide patients into several unequal groups: the largest group includes patients with only signs of coronavirus pneumonia (83.3 (95% CI 79.7–87.3%)); patients with a combination of COVID-19 and different concomitant pathologies (10.2 (95% CI 7.4–13.6%)); and significantly smaller groups — patients with signs of COVID-19 and its complications (pleural effusion, secondary bacterial pneumonia, destruction, pneumothorax) — 3.4 (95% CI 1.7–5.4%); patients with another disorders (0.6 (95% CI 0–1.4%)) or without abnormal CT signs (2.5 (95% CI 0.8–4.5%)), Figure 1.

Here are clinical examples demonstrating the role of the chest CT in the diagnosis of COVID-19, its complications and associated disorders.

Clinical Cases

Male patient X., 32

The patient was hospitalized on the 8th day of disease in the TRC with the following diagnosis: “Suspected coronavirus disease, bilateral polysegmental pneumonia, RF stage 2. Hypertensive disease, stage II. Arterial hypertension stage 2. Risk 2 (medium). Target BP < 130/ < 80 mm Hg. Obesity grade II (BMI 38.6 kg/m²). NEWS (Protocol for assessing the severity of the patient’s condition) score 5.” C-reactive protein (CRP) 92 mg/l, lactate dehydrogenase (LDH) 1,470 U/l.

CT at admission (Figure 2A) showed multiple separate and confluent areas of ground-glass opacity in

all pulmonary fields and peribronchovascular and subpleural areas, almost symmetrically. Confluent lesions (up to 6–8 cm) were found apically, in the middle lobe, as well as in posterior-basal segments of both lungs (an arrow marks a focus in S2 of the right lung). In connection with the lesions, a reticular component and linear cord-like thickening were determined; no consolidation visible. The size of the lung lesion was 50–75% (CT-3 according to the recommended express form for the description of thoracic CT results of a patient with suspected COVID-pneumonia), CO-RADS 5.

Treatment was started (hydroxychloroquine, azithromycin, amoxicillin + clavulanic acid); positive PCR result on SARS-CoV-2 RNA was obtained. Due to increased intoxication and RF, the patient was transferred to an intensive care unit. High-flow oxygen therapy was conducted; tocilizumab 800 mg i.v. was administered once. On the 11th of the disease, the patient was intubated, artificial ventilation (AV) was started. On the 12th day, percutaneous dilation tracheostomy was performed, complicated by rapidly resolved pneumothorax and subcutaneous emphysema.

Fever persisted. Repeated CT performed on the 16th day of the disease (Figure 2B) revealed enlarged ground-glass opacity zones in both lungs, most significant in S8–S10; a consolidation zone appeared in S2 of the right lung (marked by an arrow). The lesion was more than 75% (CT-4). ARDS pattern.

The bacteriological test of bronchopulmonary lavage revealed *Klebsiella pneumoniae*. The repeated PCR study found no SARS-CoV-2 RNA.

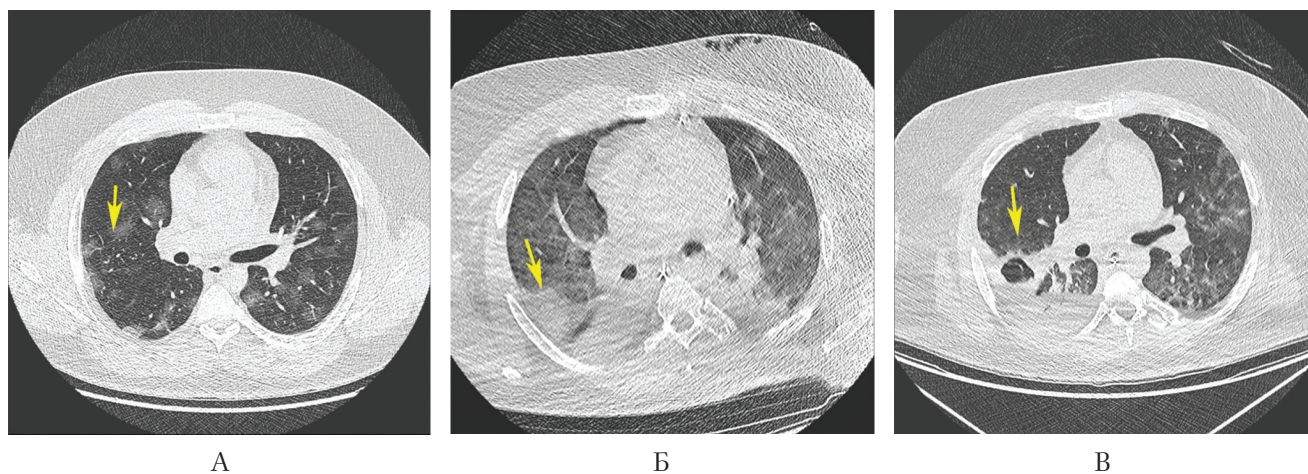


Figure 2. Follow-up of CT imaging of 32 y.o. patient with confirmed COVID-19 pneumonia, acute respiratory distress syndrome and cavitation and consolidation with cavitation in the right lung

Subsequently, antibacterial treatment, adjusted based on the sensitivity of microflora, resulted in the stabilization of the patient's condition. Nevertheless, CT performed on the 30th day of the disease, with an underlying increase in alveolar consolidation in the upper and lower lobes of the right lung and new small areas of consolidation appeared in the upper lobe of the left lung, revealed a lung cavity, 14 mm in size, surrounded by a ring-like consolidation in the middle lobe of the right lung (abscess development).

On the 39th day of the disease, alveolar consolidation zones significantly decreased, while areas of ground-glass opacity remained; no new foci of consolidation were visible. The lung cavity, 17 mm in size, in the middle lobe of the right lung remained; in S2 from the right, in the conditions of massive consolidation, lung cavities were visible, up to 32 x 20 mm in size that drained into a subsegmental bronchus (Figure 2B). A small amount of effusion in the right pleural cavity.

Despite the treatment performed, the patient suffered a cardiac arrest; he was successfully resuscitated. However, severe hypoxia led to the patient's vegetative state. Considering positive changes in the clinical and laboratory picture of ARDS, bilateral abscessed pneumonia, and the absence of SARS-CoV-2 RNA in oropharyngeal swabs, the patient was transferred to another medical institution for rehabilitation.

Therefore, repeated CT allowed to diagnose a secondary bacterial infection with subsequent

abscessing in a patient with severe coronavirus pneumonia that required using an immunosuppressive drug, a prolonged stay in an intensive care unit, artificial ventilation, and tracheostomy.

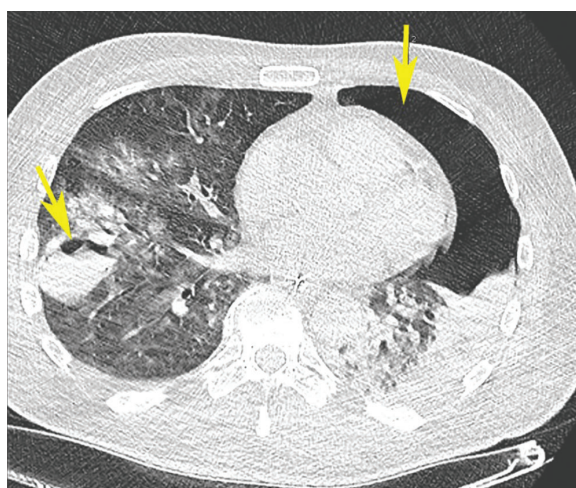
Male patient T., 58

Onset with fever up to 39.5 °C during 5 days, dry cough, shortness of breath. Coronavirus swab test was conducted in an outpatient setting; SARS-CoV-2 RNA was detected. Symptomatic treatment was performed, with no effect. The patient was urgently hospitalized on the 6th day of the disease. On admission: Severe condition. Body temperature: 39.5 °C. Awake, in control. RR 22/min. Saturation 93%. HR 90 bpm. NEWS score 6.

CT on admission: in the parenchyma of both lungs there are multiple areas of ground-glass opacity combined with minimal reticular changes (CO-RADS 5, CT-2).

Treatment was started (hydroxychloroquine, azithromycin, amoxicillin + clavulanic acid, enoxaparin), as well as oxygen therapy.

On the 8th day of the disease, due to increasing RF, saturation decreased to 89%, dyspnea increased to 30 bpm; the patient was transferred to the intensive care unit and intubated; artificial ventilation was started, followed by tracheostomy. On the 18th day of the disease, due to a sharp decrease in oxygenation, CT was performed and left-sided pneumothorax was found (Figure 3 A, B); therefore, the pleural cavity was drained. With underlying ground-glass opacity, there is consolidation



A



B

Figure 3. CT scans of 58 y.o. patient with confirmed COVID-19 and bacterial pneumonia, ventilator-associated pneumothorax in the left lung and consolidation with cavitation in the right lung

with a lung cavity (arrow) in the lower lobe of the right lung and a left-sided pneumothorax (arrow). On the left side — ground-glass opacity in a partially compressed lung parenchyma as a result of the mass effect due to air in left pleural cavity.

In connection with the treatment performed, the patient's condition improved; he was taken off oxygen therapy, decannulated, and transferred to the ward. There were no complications during the subsequent recovery period; the patient was discharged in satisfactory condition on the 51st day from the disease onset.

In this clinical case, CT allowed us to monitor changes in the lungs in a patient who was in the intensive care unit for a long time due to severe coronavirus disease complicated by pneumonia, bacterial superinfection with the destruction of

lung tissue, and a pneumothorax, most likely associated with artificial ventilation.

Female patient A., 79

At the beginning of April 2020, she was treated for community-acquired pneumonia in a hospital (not TRC); SARS-CoV-2 RNA was twice not found in smears from the oral cavity and nasopharynx. Comorbidities: Hypertensive disease stage III. Arterial hypertension stage 2. Risk 4 (very high). Target BP < 130 / < 80 mm Hg, cerebrovascular disease, consequences of stroke of unknown age, Parkinson's disease. Class I obesity grade (BMI 31 kg/m²). CT results revealed large unilateral infiltration in the hilar region of the left lung with indistinct contours, typical for bacterial pneumonia. Over time — infiltration completely regressed

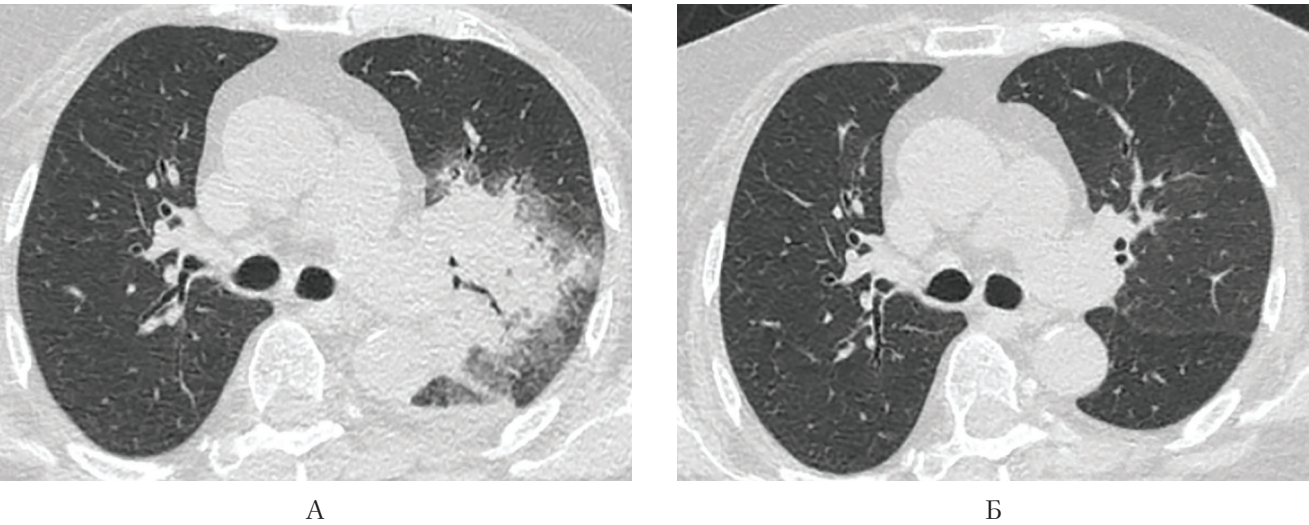


Figure 4. Regress of CT lesions in 79 y.o. patient with community acquired pneumonia

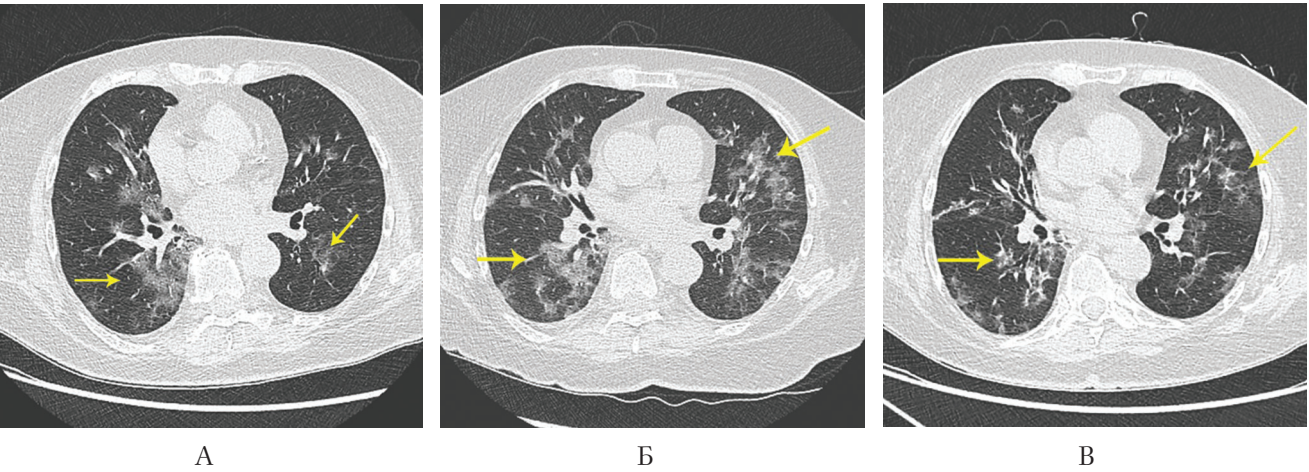


Figure 5. Same patient, 1-21 days after convalescence after bacterial pneumonia. Extent and partial absorption of CT signs of confirmed COVID-19 pneumonia

into S1 + 2 of the left lung (Figure 4 A and B). The patient was discharged with improvement.

The day after discharge, the patient's body temperature rose to 38 °C. As a result, she was hospitalized in the TRC. On admission, she was in a state of moderate severity, with forced attitude due to restricted mobility. No rales were heard. SpO₂ — 94%. Nasopharyngeal swab test revealed SARS-CoV RNA.

Chest CT at admission (Figure 5A): in the parenchyma of both lungs, there are multiple diffuse areas of decreased airiness of lung tissue in the form of ground-glass opacity located in the hilar and subpleural zones, the largest one in S6 of the right lung (up to 55 x 32 mm) (CO-RADS 5, CT-2). During the next few days, her state deteriorated, lung damage increased to the CT-3 stage (Figure 5 B). After stabilization and partial regression of inflammation (Figure 5B), the patient was discharged on the 21st day of hospitalization.

Therefore, assessing the data on patient A., we can assume that the first episode of pneumonia (probably hypostatic) was associated with bacterial infection, and the second episode — with coronavirus infection.

Female patient S., 58

In 2005, she underwent radical mastectomy with lymphadenectomy on the left side for breast cancer, followed by polychemotherapy and radiation therapy.

On April 30, 2020, she was hospitalized (not at TRC) due to shortness of breath with minor physical exertion. Anthracycline cardiomyopathy was diagnosed. The diagnosis also included: Left bundle branch block. First-degree atrioventricular block. CHF with reduced LV EF (left ventricular ejection fraction 26%) stage IIB FC III. Bilateral hydrothorax. Pleural effusion was evacuated, treatment for CHF was prescribed. The patient was discharged with improvement. A week after discharge, febrile body temperature appeared, shortness of breath worsened. CT was performed in the local clinic at the place of residence. It revealed that with underlying cardiomegaly, both lungs had multiple inductions of the ground-glass opacity type, polysegmental, mostly peripherally located, with signs of consolidation, 50–75% on the right and 25–50% on the left side. The patient was hospitalized in the TRC in a severe state with dyspnea at rest.

On admission: Body temperature 36.1 °C. Diffuse cyanosis. RR 22–24 per minute. SpO₂ 94%, with oxygen therapy — 98–100%. BP 100/60 mm Hg on both arms, HR 125 bpm, on ECG — wide complex tachycardia (compensated with drugs). No edemas or hepatomegaly. NEWS score 8. Nasopharyngeal swab test revealed SARS-CoV RNA.

Chest CT at admission: in the parenchyma of both lungs, there is a diffuse induration of the interlobular interstitium (interstitial edema), with associated extended and confluent areas of ground-glass opacity in the parenchyma, primarily basal and on the right side (50–75% on the right, 25–50% on the left, CT-3, CORADS 4). Infiltration areas about 14 mm in size are also visible; there is a subpleural area measuring 55 x 11 x 44 mm in the apex of the left lung. Pleural effusion — thickness of the fluid layer on the left side — 3 cm, on the right side — 1.3 cm. Cardiomegaly. (Figure 6).

Due to the severe cardiac disorder, it was decided not to use hydroxychloroquine, azithromycin, lopinavir/ritonavir. Amoxicillin + clavulanic acid were prescribed, followed by cefoperazone + sulbactam. On the 11th day of the disease, a repeated chest CT revealed a decrease in the size and number of reduced pneumatization areas according to the type of consolidation/ground-glass opacity in both lungs down to 35% (CT-2). At the same time, there was an increase in the severity of interlobular interstitial thickening, the amount of free fluid in pleural cavities (up to 4 cm on the right and 5.5 cm on the left), and the compression of the lower lobes. The volume of S1 + 2 of the left lung decreased due to the subpleural zone of fibrosis (Figure 7).

Treatment was intensified (diuretic therapy, intravenous administration of albumin, considering hypoalbuminemia).

Chest CT on the 18th day of the disease showed a further decrease in the size and number of consolidation/ground-glass opacity areas in both lungs to 25%. Signs of congestion in pulmonary circulation decreased; however, the amount of fluid in pleural cavities increased slightly (Figure 8).

The patient was discharged with significantly decreased dyspnea (SpO₂ 98%), stable hemodynamics (ECG: sinus rhythm with HR 78 bpm, BP 90/60 mm Hg), decrease in CRP level from 49.9 to 1.6 mg/l after two negative swab tests for SARS-CoV-2. The patient subsequently underwent elective cardiac resynchronization therapy.

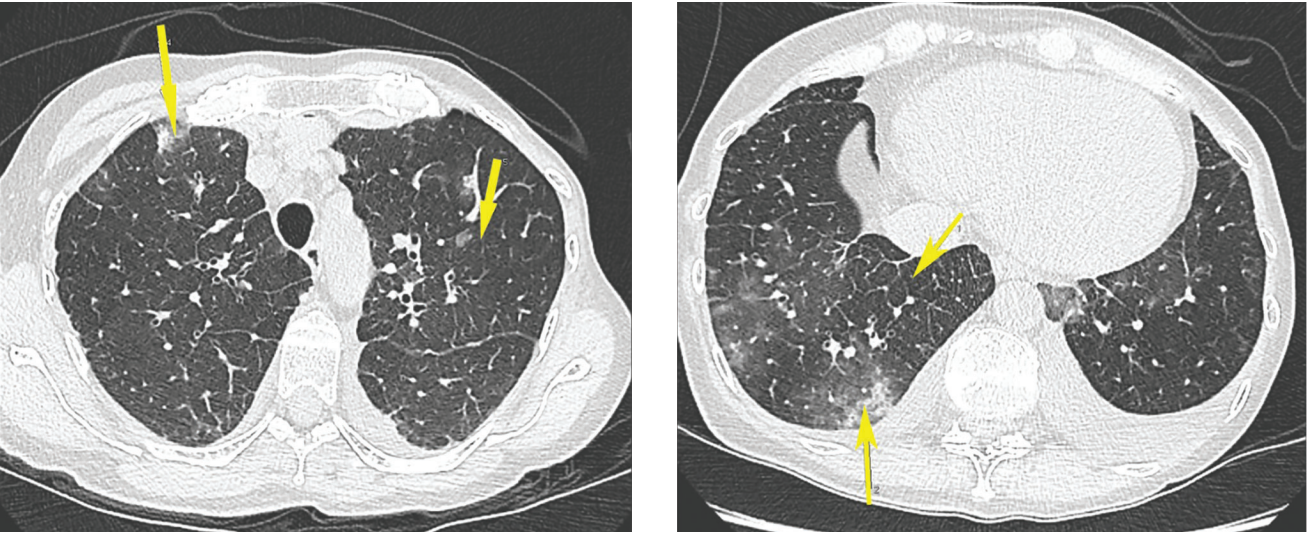


Figure 6. CT scans of 58 y.o. patient with anthracycline cardiomyopathy (cardiomegaly), decompensated heart failure (Kerley lines) and confirmed COVID-19 pneumonia (ground glass opacities) at admission

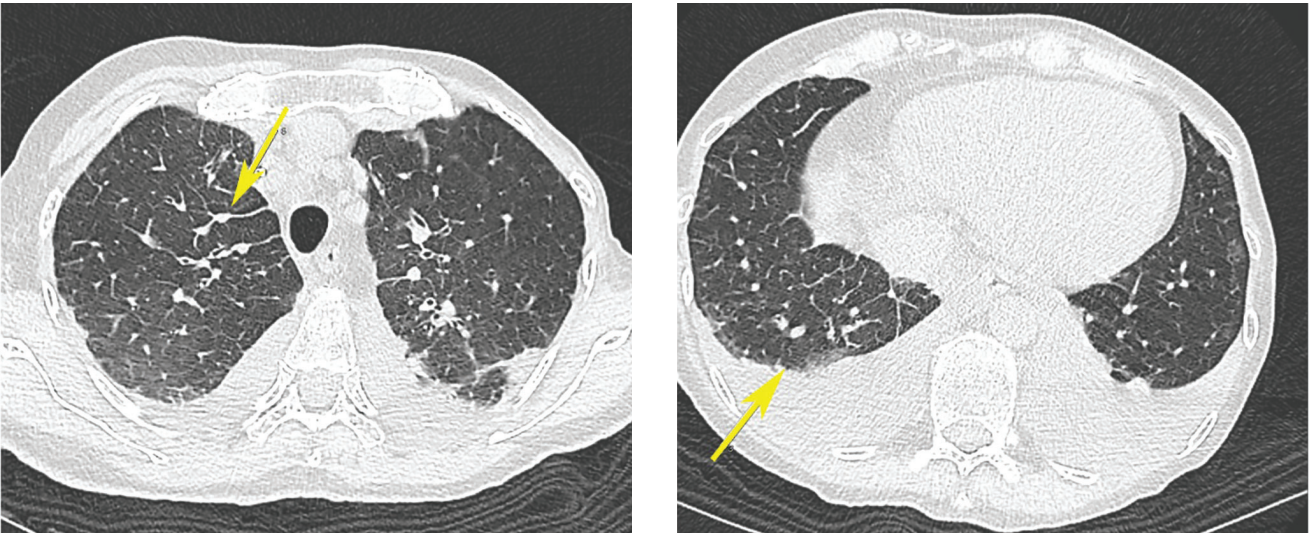


Figure 7. Same patient, 11 day of disease. Marked pleural effusion

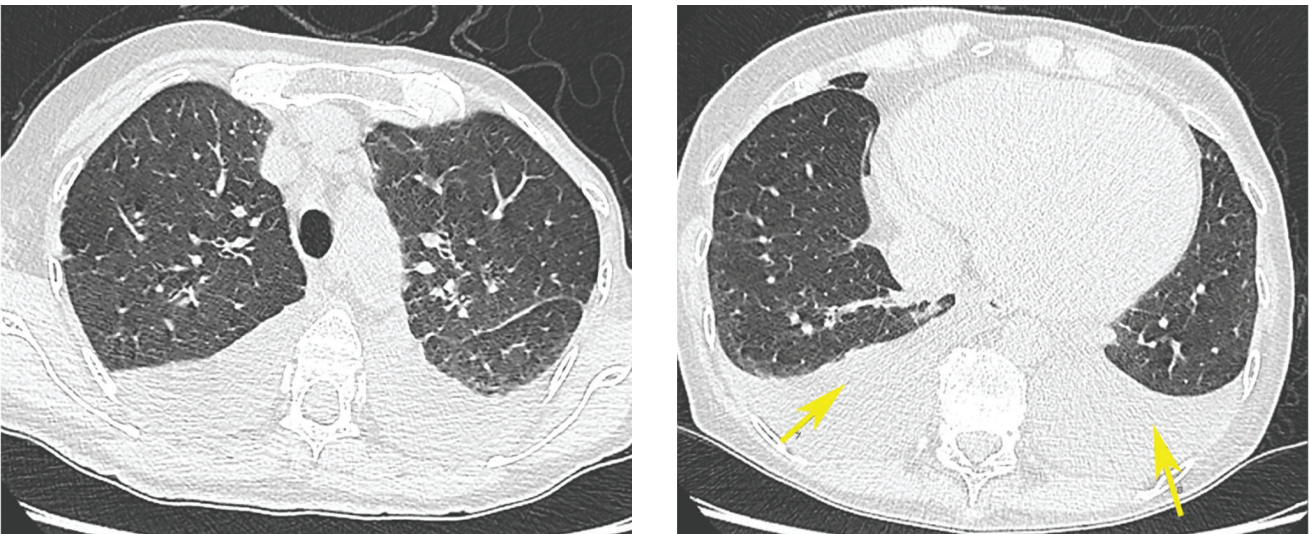


Figure 8. Same patient, 18 day of disease. Partial regress of pneumonia and lung edema signs. Slight increase of pleural effusion

In this clinical case, CT allowed us to perform differential diagnostics of coronavirus infection-induced infiltration from signs of congestion in pulmonary circulation in a patient with severe concomitant heart failure and postradiation changes in the lung parenchyma.

Pulmonary edema is a common cause of the rapid development of ground-glass opacity areas, which usually grow centrifugally, as opposed to the typical picture of COVID-19. This is usually accompanied by other typical signs (thickening of the interlobular septa, hydrothorax, and dilation of pulmonary veins [22]). In young patients with COVID-19 without concomitant cardiac pathology, pulmonary edema may be a manifestation of acute myocarditis [23]. Diffuse areas of ground-glass opacity can also develop with intralveolar hemorrhage due to vasculitis. Their subpleural location is also not typical, unlike COVID-19. In cases of Goodpasture syndrome, such a CT picture is accompanied by hemoptysis and acute renal damage [24]. Another reason for subpleural zones of ground-glass opacity is drug-induced pneumonitis, which manifests as non-specific interstitial pneumonia [25].

Female patient K., 87

The patient lives with her granddaughter who has had coronavirus disease. She considers herself ill for about a month when she complained of weakness and developed a dry cough. The patient

was hospitalized at the local clinic after CT that revealed multisegmental interstitial changes in the parenchyma (Co-RADS 5, CT-3). State at admission was satisfactory, 0 points on the NEWS scale. Temperature 36.5 °C. SpO₂ 96%. Laboratory test results: hemoglobin 98 g/l, hematocrit 31.0%, RBC — $3.9 \times 10^{12}/l$, WBC $8 \times 10^9/l$ (lymphocytes 10%, monocytes 10%), LDH 551 U/l, C-reactive protein 196.4 mg/l. She was hospitalized since she falls in the risk group (senile age, hypertensive disease). Smears from the oropharynx for RNA SARS-CoV-2 returned 4 negative results.

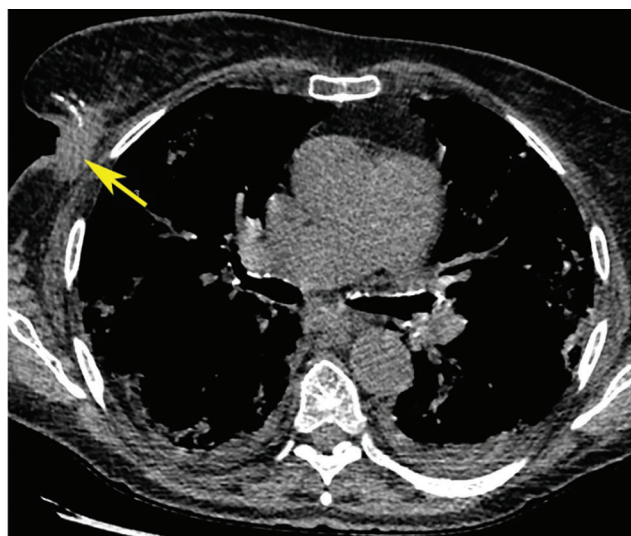
CT, in addition to multiple ground-glass opacity areas with small consolidation elements in the parenchyma of both lungs, primarily subpleural (about 60% of pulmonary parenchyma affected), shows a mass of the right breast, with indistinct contours, 18.5×36.5×41 mm (Figure 9).

During the follow-up period, the CRP level decreased to 16.4 mg/l. CT showed moderate positive changes (a decrease in the size of ground-glass opacity areas in both lungs, development of consolidation zones in their projection, slightly decreased damage volume within CT-3).

Therefore, considering the duration of complaints, negative test results for SARS-CoV-2 RNA, and CT data, it can be assumed that the patient was infected with coronavirus more than a month ago. The disease had few symptoms, and the patient was hospitalized when virus replication had already stopped.



A



B

Figure 9. 87 y.o. patient, hospitalized with viral pneumonia (highly likely COVID-19 despite negative PCR) and first identified breast tumor

However, changes in the lungs caused by the coronavirus infection and found on CT scans remained. CT made it possible to identify a breast neoplasm that was not previously diagnosed (including in an outpatient setting).

Female patient A., 51

Onset of disease with high body temperature of up to 38.3 °C, anosmia, cough. On the 5th day of the disease, the patient was hospitalized (not at TRC). Chest CT revealed bilateral pneumonia (CT-3, Figure 10 A, B); coronavirus etiology was confirmed by laboratory tests. Antibacterial

therapy was prescribed (amoxiclav, azithromycin), hydroxychloroquine. On the 17th day of the disease, after temperature normalization, the patient was discharged. Over the next three weeks, there was no increase in temperature, but chest discomfort and weakness persisted.

Control chest CT was performed in an outpatient setting (Figure 11A). Diffuse areas of reduced airiness of the parenchyma of the ground-glass opacity type remained, which occupy most of the parenchyma (about 75%); this information was interpreted as a recurrence of coronavirus pneumonia. The patient was hospitalized at the TRC.

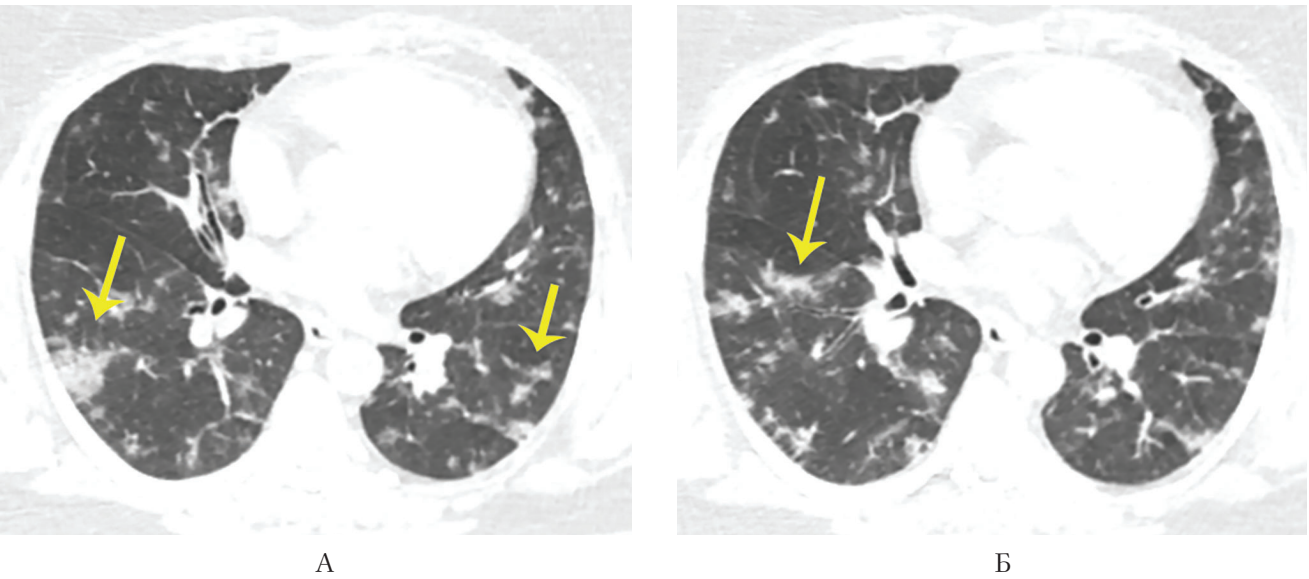


Figure 10. CT scans of 51 y.o. patient with confirmed COVID-19 pneumonia. 5th day after onset of symptoms

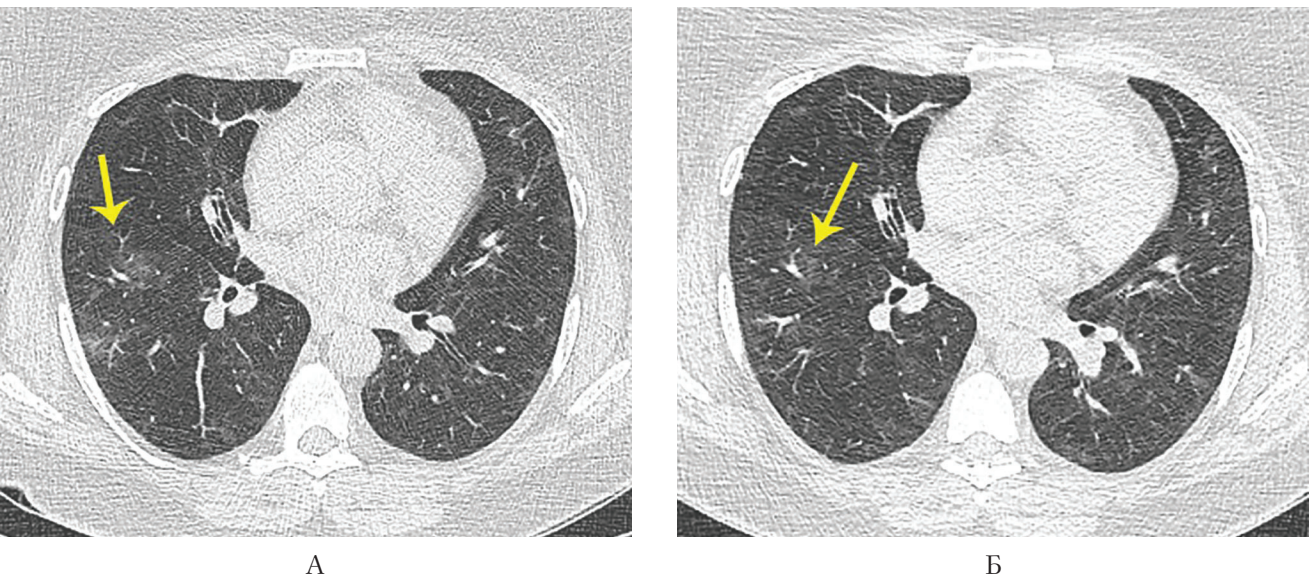


Figure 11. Ame patient, 3 weeks after discharge. Re-hospitalized with residual symptoms and ground glass opacities at CT scan

Upon admission, her state was satisfactory, no catarrhal symptoms, cough, fever, and no signs of RF. Laboratory test results: WBC $10.1 \times 10^9/l$, albumin 38.2 g/l, LDH 324 U/l, C-reactive protein 4.4 mg/l. SARS-CoV-2 RNA was not found in oropharyngeal swabs twice. No antiviral or antibacterial drugs were prescribed. Antithrombotic prevention was conducted.

Due to the absence of febrile intoxication syndrome, laboratory test results and CT data were regarded as residual manifestations of coronavirus pneumonia. On the 5th day of hospitalization, chest CT was repeated, no significant changes were found (Figure 11B). The patient was discharged on the 6th day of hospitalization; consultation with a pulmonologist is recommended, as well as follow-up examination in 1 month.

This example demonstrates the possibility of long-term persistence of changes detected during CT after coronavirus pneumonia. Only long-term and large-scale studies will determine who among patients who have suffered COVID-19 will have such changes, how long they will persist, their origin, clinical and epidemiological significance. Before systematizing data, such changes in the CT scan should be evaluated jointly by a radiologist and a clinician for each patient individually, taking into account the history of the patient's disease, clinical status, and laboratory test results.

Male patient F., 51

In February 2020, chest CT revealed mediastinal liposarcoma with signs of spreading to the right

pleural cavity. In April, the patient was hospitalized (not at TRC) and had contact with COVID-19 patients. He subsequently complained of weakness, cough, dyspnea, and temperature rise to 37.8 °C. As a result, MSCT was performed, which revealed subpleural foci of the ground-glass opacity type, with a thickened intralobular interstitium. The patient was transferred to the TRC. On admission — SpO₂ 98%, NEWS score 0.

CT of lungs performed in the inpatient department of TRC revealed multiple ground-glass opacity areas (CO-RADS 4, CT4) in the left lung, polysegmental, with most of the damage in the peripheral parts. When comparing with the previous CT, new ground-glass opacity areas were visible in the same lung, in segments 5 and 8. A large mediastinal mass lesion of solid fat-density of the same size of 124 × 82 × 90 mm persisted (Figure 12A).

Treatment with hydroxychloroquine, azithromycin, enoxaparin in prophylactic doses and omeprazole was started.

After 5 days, CT of lungs showed positive changes in the form of a decrease in the size and number of ground-glass opacity areas in the left lung and the transformation of some of them into linear fibrosis. Mediastinal mass lesion without negative changes (Figure 12B).

In the course of treatment, the patient's body temperature returned to normal; there were no catarrhal symptoms or signs of respiratory failure. Laboratory signs of inflammation regressed, PCR for SARS-CoV-2 RNA returned a negative result three times.

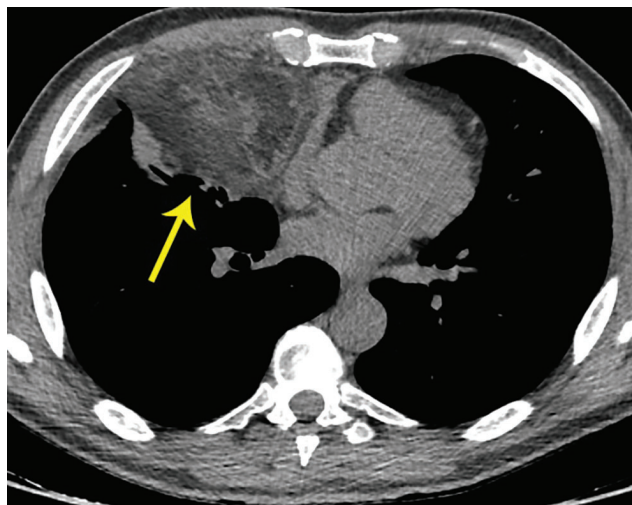
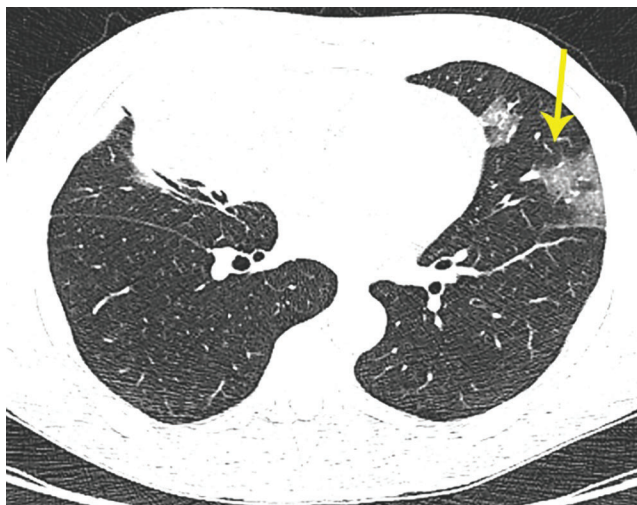


Figure 12. 51 y.o. patient with mediastinal liposarcoma, hospitalized with clinical and CT signs of COVID-19

Despite the negative PCR test results, the combination of epidemiological data with a typical clinical and CT picture, typical for pneumonia caused by COVID-19 infection, the correct treatment strategy with a positive result was chosen.

Conclusion

In the context of the novel coronavirus pandemic, one of the primary tasks solved by CT is the diagnosis of COVID-19 when the SARS-CoV-2 RNA test is inaccessible or negative. No less important is the ability of CT to monitor changes in lung tissue in patients with COVID-19 for timely adjustment of the treatment strategy.

In addition to monitoring changes typical for COVID-19, the CT in clinical practice allows differential diagnosis of pulmonary and extrapulmonary disorder in comorbid patients. Our experience shows that the combination of coronavirus pneumonia with another disease of the chest organs occurs in 10.2% of patients; 0.6% exhibit only radiological symptoms of other diseases without signs of coronavirus infection.

It is advisable to conduct a primary CT in all patients with suspected COVID-19 and a repeated CT if there is no clinical improvement during 7 days of treatment or if clinical and laboratory parameters worsen.

Author Contribution:

All the authors contributed significantly to the study and the article, read and approved the final version of the article before publication.

Petrovichev V.S. (ORCID ID: <https://orcid.org/0000-0002-8391-2771>): research concept

and design, data collection and processing, writing article, article editing, placing an article on the journal site.

Melekhov A.V. (ORCID ID: <https://orcid.org/0000-0002-1637-2402>): data collection and processing, statistical data processing, writing article

Sayfullin M.A. (ORCID ID: <https://orcid.org/0000-0003-1058-3193>): research concept

and design, data collection.

Nikitin I.G. (ORCID ID: <https://orcid.org/0000-0003-1699-0881>): research concept and design, writing article, editing

Список литературы/ References:

1. Undiagnosed pneumonia — China (Hubei): request for information. [Электронный ресурс]. URL: <https://promedmail.org/promed-post/?id=6864153>. (дата обращения: 11.06.2020).
2. «Novel Coronavirus — China». World Health Organization (WHO). 12 January 2020. [Электронный ресурс]. URL: <https://www.who.int/csr/don/12-january-2020-novel-coronavirus-china/en/>. (дата обращения: 11.06.2020).
3. Tan W., Zhao X., Ma X., et al. A novel coronavirus genome identified in a cluster of pneumonia cases — Wuhan, China 2019–2020. *China CDC Weekly* 2020; 2(4):61–62. doi:10.46234/ccdcw2020.017.
4. Verdecchia P., Cavallini C., Spanevello A., et al. The pivotal link between ACE2 deficiency and SARS-CoV-2 infection. *European Journal of Internal Medicine*. 2020; 76: 14–20. doi:10.1016/j.ejim.2020.04.037.
5. Zhu N., Zhang D., Wang W., et al. A Novel Coronavirus from Patients with Pneumonia in China, 2019. *N Engl J Med*. 2020; 382(8):727–733. doi:10.1056/NEJMoa2001017.
6. Gorbalenya A.E., Baker S.C., Baric R.S., et al. The species Severe acute respiratory syndrome-related coronavirus: classifying 2019-nCoV and naming it SARS-CoV-2. *Nature Microbiology*. 2020;5(4):536–544. doi:10.1038/s41564-020-0695-z.
7. Guan W., Ni Z., Hu Y., et al. Clinical Characteristics of Coronavirus Disease 2019 in China. *N Engl J Med*. 2020; 382:1708–1720. doi:10.1056/NEJMoa2002032.
8. Pan F., Ye T., Sun P., et al. Time Course of Lung Changes at Chest CT during Recovery from Coronavirus Disease 2019 (COVID-19). *Radiology*. 2020;295(3):715–21. doi: 10.1148/radiol.202000370.
9. Сперанская А.А. Лучевые проявления новой коронавирусной инфекции COVID-19. Лучевая диагностика и терапия. 2020;11(1):18–25. doi:10.22328/2079-5343-2020-11-1-18-25. Speranskaya A.A. Radiological signs of a new coronavirus infection COVID-19. Diagnostic radiology and radiotherapy. 2020;11(1):18–25. [In Russian]. doi:10.22328/2079-5343-2020-11-1-18-25.
10. Dai WC, Zhang HW, Yu J. CT Imaging and Differential Diagnosis of COVID-19. *Can Assoc Radiol J*. 2020. Mar 4; 846537120913033. Doi: 10.1177/0846537120913033.
11. Fang Y., Zhang, H., Xie, J. Sensitivity of Chest CT for COVID-19: Comparison to RT-PCR. *Radiology*. 2020 296(2):E115–E117. doi: 10.1148/radiol.202000432.

12. Профилактика, диагностика и лечение новой коронавирусной инфекции (COVID-19). Версия 8 Временные методические рекомендации. Утверждены заместителем Министра здравоохранения Российской Федерации 3.09.2020 г. [Электронный ресурс]. URL: https://static-0.minzdrav.gov.ru/system/attachments/attaches/000/051/777/original/030902020_COVID-19_v8.pdf. (дата обращения: 24.09.2020).
Prevention, diagnosis and treatment of new coronavirus infection (COVID-19). Version 8 Temporary guidelines. Approved by the Deputy Minister of Health of the Russian Federation on 09.03.2020 [Electronic resource]. URL: https://static-0.minzdrav.gov.ru/system/attachments/attaches/000/051/777/original/030902020_COVID-19_v8.pdf. (of the application: 24.09.2020). [In Russian].
13. He G., Wu J., Shi J., et al. COVID-19 in Tuberculosis patients: a report of three cases. *J Med Virol*. 2020;10.1002/jmv.25943. doi:10.1002/jmv.25943.
14. Zhu W.J., Wang J., He X.H. The differential diagnosis of pulmonary infiltrates in cancer patients during the outbreak of the 2019 novel coronavirus disease. *Zhonghua Zhong Liu Za Zhi*. 2020;42(4):305-311. doi: 10.3760/cma.j.cn112152-20200303-00166.
15. Социально значимые заболевания населения России в 2018 году (Статистические материалы). Министерство здравоохранения Российской Федерации. Департамент мониторинга, анализа и стратегического развития здравоохранения. ФГБУ «Центральный научно-исследовательский институт организации и информатизации здравоохранения» Минздрава России. Материал опубликован 31.07.2019г. [Электронный ресурс]. URL: <https://www.rosminzdrav.ru/ministry/61/22/stranitsa-979/statisticheskie-i-informatsionnye-materialy/statisticheskiy-sbornik-2018-god>. (дата обращения: 13.06.2020).
Social significant diseases of the population of Russia in 2018 (Statistical materials). Ministry of Health of the Russian Federation. Department of monitoring, analysis and strategic development of health care. FSBI "Central Research Institute for Organization and Informatization of Health Care" of the Ministry of Health of Russia. Published on July 31, 2019. [Electronic resource]. URL: <https://www.rosminzdrav.ru/ministry/61/22/stranitsa-979/statisticheskie-i-informatsionnye-materialy/statisticheskiy-sbornik-2018-god>. (date of the application 11.06.2020). [In Russian].
16. О состоянии санитарно-эпидемиологического благополучия населения в Российской Федерации в 2018 году: Государственный доклад. М.: Федеральная служба по надзору в сфере защиты прав потребителей и благополучия человека, 2019; 254 с. ISBN 978–5–7508–1681–1
About of sanitary and epidemiological well-being of the population in the Russian Federation in 2018: State report. Moscow: Federal Service for Supervision of Consumer Rights Protection and Human Welfare, 2019; 254 p. ISBN 978–5–7508–1681–1. [In Russian].
17. Pan F., Ye T., Sun P., Gui S., Liang B., Li L. Time course of lung changes on chest CT during recovery from 2019 novel coronavirus (COVID-19) Pneumonia. *Radiology*. 2020 doi: 10.1148/radiol.2020200370.
18. Kligerman S.J., Franks T.J., Galvin J.R. From the Radiologic Pathology Archives: Organization and fibrosis as a response to lung injury in diffuse alveolar damage, organizing pneumonia, and acute fibrinous and organizing pneumonia. *Radiographics*. 2013;33:1951–1975.
19. Bai H.X., Hsieh B., Xiong Z., Halsey K., Choi J.W., Tran T.M. L. Performance of radiologists in differentiating COVID-19 from viral pneumonia on chest CT. *Radiology*. 2020 doi: 10.1148/radiol.2020200823.
20. Caruso D, Polidori T, Guido G, Nicolai M, Bracci B, Cremona A, Zerunian M, Polici M, Pucciarelli F, Rucci C, Dominici C, Girolamo MD, Argento G, Sergi D, Laghi A. Typical and atypical COVID-19 computed tomography findings. *World J Clin Cases*. 2020 Aug 6;8(15):3177-3187. doi: 10.12998/wjcc.v8.i15.3177
21. Prokop M., van Everdingen W., van Rees Vellinga T, et al. CO-RADS — A categorical CT assessment scheme for patients with suspected COVID-19: definition and evaluation. *Radiology*. 2020;201473. doi:10.1148/radiol.2020201473.
22. Hani C, Trieu NH, Saab I, Dangeard S, Bennani S, Chasagnon G, Revel MP. COVID-19 pneumonia: A review of typical CT findings and differential diagnosis. *Diagn Interv Imaging*. 2020 May;101(5):263-268. doi: 10.1016/j.diii.2020.03.014
23. Chen C., Zhou Y., Wang D.W. SARS-CoV-2: a potential novel etiology of fulminant myocarditis. *Herz*. 2020/
24. Cordier J.-F., Cottin V. Alveolar hemorrhage in vasculitis: primary and secondary. *Seminars in Respiratory and Critical Care Medicine*. 2011; 32: 310–321.
25. Rossi S.E., Erasmus J.J., McAdams H.P., Sporn T.A., Goodman P.C. Pulmonary drug toxicity: radiologic and pathologic manifestations. *Radiographics*. 2000; 20: 1245–1259.